Liquid Crystals
Publication details, including instructions for authors and subscription information:
http://www.informaworld.com/smpp/title~content=t713926090

Mesogenic derivatives of 2S,3S-2-halogeno-3-methylpentanoic acid with helix twist inversion in the smectic C* phase

J. Szydlowska; D. Pociecha; J. Matraszek; J. Mieczkowski

Online publication date: 06 August 2010

To cite this Article Szydlowska, J. , Pociecha, D. , Matraszek, J. and Mieczkowski, J.(1999) 'Mesogenic derivatives of 2S,3S-2-halogeno-3-methylpentanoic acid with helix twist inversion in the smectic C* phase', Liquid Crystals, 26: 12, 1787 — 1796
To link to this Article: DOI: 10.1080/026782999203418
URL: http://dx.doi.org/10.1080/026782999203418

LIQUID CRYSTALS, 1999, VOL. 26, NO. 12, 1787–1796

Mesogenic derivatives of 2S,3S-2-halogeno-3-methylpentanoic acid with helix twist inversion in the smectic C* phase

J. SZYDŁOWSKA*, D. POCIECHA

Laboratory of Dielectrics and Magnetics, Chemistry Department, Warsaw University, Al. Żwirki i Wigury 101, 02-089 Warsaw, Poland

J. MATRASZEK and J. MIECZKOWSKI

Laboratory of Natural Compound Analysis, Chemistry Department, Warsaw University, ul. Pasteura 1, 02-093 Warsaw, Poland

(*Received 7 May 1999; accepted 27 July 1999*)

Two homologous series of chloro and bromo derivatives of *S*,*S*-3-methylpentanoic acid were synthesized and studied. For some of these compounds an inversion of helix twist sense in the smectic C* phase was observed. Dielectric dispersion measurements showed a pronounced anomaly of the Goldstone mode relaxation frequency and strength close to the helix inversion point. Moreover, a qualitative difference in behaviour of the mode in samples with planar and with homeotropic alignment was detected; this is due to surface interactions.

1. Introduction

A few compounds have been found that exhibit spontaneous twist sense inversion of the helical superstructure in the SmC* phase [1–3]. This phenomenon implies that at a certain temperature the helix is infinitely long, and a state with nearly uniform tilt direction is reached. At this temperature the elastic torque is weak and as a result the Goldstone mode, which characterizes collective tilt angle phase fluctuations, should slow down [4]. It is also expected that the Goldstone mode strength should maximize. However, this behaviour has not yet been confirmed experimentally.

The nature of the twist inversion phenomenon is still not clear. There are two basic hypotheses that describe it quantitatively. The first is based on a phenomenological model of the free energy and stresses the role of a temperature-dependent value of the ratio of tilt to spontaneous polarization [5]. The second emphasizes the role of competition between different conformers of the molecules [6]. Changes of conformer relative population might lead to the helical inversion, particularly in compounds with several chiral centres.

In this communication we describe two new series of mesogenic derivatives of 2*S*,3*S*-2-halogeno-3-methylpentanoic acid with two chiral centres that were especially designed to show the helix twist inversion and enable investigations of the dielectric perperties of the chiral smectic state with the unwound helix. Besides the dielectric properties, results on other basic characteristics of the materials studied, namely the phase sequence, spontaneous polarization and tilt angle values, will be given.

2. Experimental

The sequences of phases were identified by texture observations made with a Nikon Optiphot-2Pol polarizing microscope equipped with a heating stage and a photometry system. The occurrence of the helical structure in the SmC* phase was confirmed by observing homeotropic textures of freely suspended thick films, as well as by the appearance of dechiralization defect lines in the focal-conic fan textures [7]. Phase transition temperatures were determined using a Perkin Elmer DSC 7 calorimeter and heating scans of 5 K min^{-1}. The handedness of the helix structure in the SmC* phase was determined in microscopic studies of freely suspended films at a temperature close to the helix inversion point. The thickness of the film was about 20 μm. Rotation (e.g. clockwise) of linearly polarized light transmitted through the film showed the twist sense of the helix (e.g. left-handed). The helix inversion temperature was taken as the middle point of the temperature range (usually a few degrees) where the optical activity disappeared and the schlieren texture was formed.

Planar samples for tilt angle, spontaneous polarization and dielectric dispersion measurements were prepared

* Author for correspondence; e-mail: jadszyd@chem.uw.edu.pl

Journal of Liquid Crystals ISSN 0267-8292 print/ISSN 1366-5855 online © 1999 Taylor & Francis Ltd
http://www.tandf.co.uk/JNLS/lct.htm
http://www.taylorandfrancis.com/JNLS/lct.htm

using glass plates carrying transparent ITO electrodes, coated with planar surfactant and rubbed, separated by Mylar spacers of various thickness—mainly 23 μm. The sample cells were filled by capillary action. The tilt angle was calculated from the difference between the extinction directions of the sample placed between crossed polarizers under opposite d.c. electric fields. Values of the spontaneous polarization were obtained from the electric current peaks recorded during $\mathbf{P}_s$ switching at a frequency of 100 Hz. The $\mathbf{P}_s$ vector, which is assumed to be collinear with the applied electric field, is positive if directed along a vector $[\mathbf{n} \times \mathbf{z}]$, where $\mathbf{n}$ is the director and $\mathbf{z}$ is the layer normal. Dielectric dispersion measurements were performed with a Wayne Kerr Precision Analyzer 6425 in the frequency range 20 Hz–300 kHz using the planar aligned samples in glass cells, as well as films suspended between metal electrodes. In the latter case, the dielectric permittivity was determined by comparison of the capacity of the LC film sample with the capacity of the same film in the isotropic phase, for which the dielectric permittivity was known from other measurements. In this procedure, the absolute value of the permittivity was obtained with some uncertainty because of the small electrode areas, but the temperature dependence of the relaxation frequency f_r and the dielectric permittivity was reflected correctly. The relaxation frequency f_r and the strength $\Delta\varepsilon$ of the dielectric mode were obtained by fitting the complex dielectric permittivity $\varepsilon^*(\bar{\omega}) = \varepsilon' - i\varepsilon''$ to the Cole–Cole dispersion law:

$$\varepsilon^* - \varepsilon_\infty = \frac{\Delta\varepsilon}{1 + (if/f_r)^{(1-\alpha)}} - i\frac{\sigma}{2\pi\varepsilon_0 f}$$

where α, ε_∞ and σ are the distribution parameter of the mode, the high frequency permittivity and the conductivity of the sample, respectively. Molecular calculations were performed using a HyperChem software package by an MM+ molecular mechanics method on a modelled fragment containing a full chiral terminal chain connected to the phenyl ring.

To confirm the molecular structure of the synthesized compounds, infrared (IR) spectra were obtained using a Nicolet Magna IR 500 spectrometer. NMR spectra were recorded on a Gemini spectrometer operating at 200 MHz for ^{1}H NMR and at 50.3 MHz for ^{13}C NMR. Tetramethylsilane (TMS) were used as an internal standard. Chemical shifts were reported in ppm. Optical rotation of chiral compounds dissolved in chloroform was measured using a Perkin-Elmer 247 MC polarimeter. TLC analyses were performed on Merck 60 silica gel glass plates and visualized using iodine vapour. Column chromatography was carried out at atmospheric pressure using Silica Gel 60 (230–400 mesh, Merck). Molecular structure was confirmed by elemental analyses.

3. Synthesis

The synthetic route to the mesogenic derivatives of 2*S*,3*S*-2-halogeno-3-methylpentanoic acid is outlined in the scheme. Some of the procedures have already been presented by Sierra *et al.* [8]. As a representative reaction sequence, the synthesis of the chloro derivative with $n = 3$ is described.

3.1. *4-Propyloxyaniline*

A mixture of 4-nitrophenol (7.25 g, 0.05 mol), propyl chloride (3.9 g, 0.05 mol), sodium iodide (7.5 g, 0.05 mol) and potassium carbonate (6.9 g, 0.05 mol) in dimethylformamide (200 ml) was heated at reflux for 10 h. Water was added to the reaction mixture and the solution was shaken with toluene (four times with 100 ml portions). The combined organic layers were dried over anhydrous magnesium sulphate, and the solvent removed by evaporation. The residue was twice crystallized from methanol. The crystals obtained were dissolved in hot ethanol (200 ml) and iron pin dust (13 g, 0.23 mol) and hydrochloric acid (1 ml 6M) were added. The mixture was heated at reflux for 4 h. The mixture was filtered and the solvent removed under vacuum. The solid residue was used in the next step without further purification.

^{1}H NMR δ 1.08 (t, 3H, $J = 7.0$ Hz), 1.73–1.81 (m, 2H), 2.25–3.37 (m, 2H), 4.03 (t, 2H, $J = 6.5$ Hz), 6.64 (d, 2H, $J = 8.3$ Hz), 6.74 (d, 2H, $J = 8.1$ Hz). ^{13}C NMR δ 16.01, 25.14, 70.23, 115.68, 116.46, 139.76, 152.37. Elemental analysis for $C_9H_{13}NO$: calc. C 71.52, H 8.61, N 9.27; found C 71.45, H 8.58, N 9.36%.

3.2. *4-Hydroxy-4'-propyloxyazobenzene*

A solution of 4-propyloxyaniline (5.0 g, 0.033 mol), hydrochloric acid (6.6 ml, 12M), water (15 ml) and tetrahydrofuran (10 ml) was stirred and cooled with an ice/water bath. To the reaction mixture, sodium nitrite (3.35 g, 0.05 mol) in water was added in small portions during 1 h; stirring was continued at 0°C for 1 h. A mixture of phenol (3.8 g, 0.04 mol) and sodium hydroxide (3.2 g, 0.08 mol) in water (100 ml) was cooled to 5°C and the solution of the diazonium salt was added. The reaction mixture was stirred for 2 h. The solution was neutralized with hydrochloric acid and then a saturated solution of sodium chloride (100 ml) was added. The precipitate was filtrated off and the crude compound purified by column chromatography on silica gel using chloroform as eluent. The product was recrystallized from hexane giving a yield of 76%.

^{1}H NMR δ 1.08 (t, 3H, $J = 7.0$ Hz), 1.75–1.84 (m, 2H), 3.68–3.79 (m, 1H), 4.08 (t, 2H, $J = 6.7$ Hz), 6.89–7.01 (m, 4H), 7.78–7.88 (m, 4H). ^{13}C NMR δ 16.01, 25.14, 70.05, 114.68, 115.77, 124.34, 124.54, 146.86, 147.20,

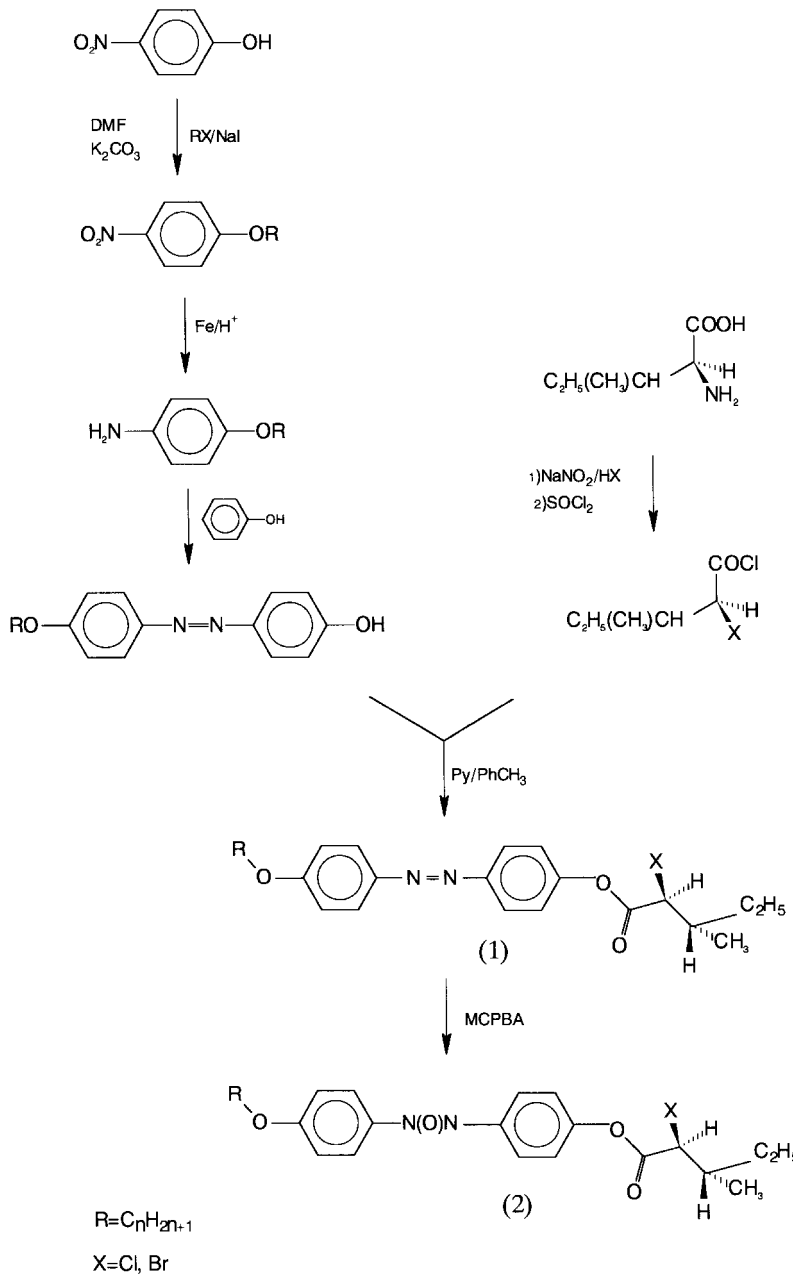

Scheme.

157.88, 161.26. Elemental analysis for $C_{15}H_{16}N_2O_2$: calc. C 70.31, H 6.25, N 10.94; found C 70.34, H 6.21, N 10.89%.

3.3. *2S,3S-2-Chloro-3-methylpentanoi c acid*

A mixture of L-isoleucine (6.55 g, 0.05 mol) and hydrochloric acid (63 ml, 6M) was stirred and cooled with an ice/water bath. After reaching 0°C, sodium nitrite (5.18 g, 0.075 mmol) was added dropwise. Vigorous stirring at 0°C was continued for 4 h. The reaction mixture was shaken five times with 100 ml portions of diethyl ether. Then the organic extracts were washed with brine and dried over anhydrous magnesium sulphate; the ether was then removed under vacuum. The crude compound was purified by column chromatography with chloroform as eluent to afford the final product (3.39 g, 0.023 mol) in 45% yield.

^{1}H NMR ($CDCl_3$) δ 0.97 (t, 3H, $J = 7.5$ Hz), 1.13 (d, 3H, $J = 6.5$ Hz), 1.33–1.50 (m, 2H), 2.16–2.27 (m, 1H), 4.40 (d, 1H, $J = 6.8$ Hz), 10.61 (s, 1H). ^{13}C NMR δ 10.80, 16.00, 25.13, 39.02, 60.12, 160.65. IR (KBr) 2985 (m), 2930 (m), 1730 (s). $[\alpha]_D^{20} = -4.80°$. Elemental analysis for $C_6H_{11}O_2Cl$: calc. C 47.84, H 7.31; found C 47.77, H 7.28%.

3.4. *2S,3S-2-Chloro-3-methylpentanoyl chloride*

A solution of 2*S*,3*S*-2-chloro-3-methylpentanoic acid (810.5 mg, 5.35 mmol) and thionyl chloride (3.5 ml) in dry toluene was heated at reflux for 3 h. Then the solvent and the excess of thionyl chloride were removed under vacuum. The crude residual product was used for the following reaction. The yield was quantitative.

3.5. *4-(4-Propyloxyphenylazoxy)phenyl 2S,3S-2chloro-3-methylpentanoate* **2**

To a stirred solution of 4-(4-propyloxyphenylazo)-phenol (937.9 mg, 4.15 mmol) and pyridine (0.35 ml, 4.15 mol) in dry toluene (50 ml), 2*S*,3*S*-2-chloro-3-methylpentanoyl chloride (909.6 mg, 5.39 mmol) dissolved in toluene (15 ml) was added dropwise. Stirring was continued at room temperature for 4 h. The product was isolated and purified by chromatography on silica gel, eluting with 30% toluene in hexane to afford compound **1** (904.0 mg, 2.33 mmol) as yellow crystals. To compound **1** (904.0 mg, 2.33 mmol), a solution of 3-chloroperbenzoic acid (483.0 mg, 2.80 mmol) in dry chloroform (50 ml) was added. The reaction mixture was left overnight at room temperature; the solvent was then evaporated under vacuum. The residue was purified by column chromatography using 50% (v/v) toluene in hexane as eluent to give the final compound (**2**) as yellow crystals (752.98 mg, 1.86 mmol) in 51% yield.

^{1}H NMR ($CDCl_3$) δ 0.99 (t, 3H, $J = 7.3$ Hz), 1.06 (t, 3H, $J = 6.9$ Hz), 1.14 (d, 3H, $J = 6.5$ Hz), 1.35–1.50 (m, 2H), 1.69–1.90 (m, 2H), 2.17–2.28 (m, 1H), 4.00 (t, 2H), 4.41 (d, 1H, $J = 6.8$ Hz), 6.93–7.00 (m, 2H), 7.21–7.28 (m, 2H), 8.20–8.37 (m, 4H). ^{13}C NMR δ 10.49, 10.89, 16.01, 22.48, 25.14, 39.04, 62.60, 70.02, 114.14, 114.31, 121.34, 121.48, 123.65, 124.01, 126.93, 128.15, 137.56, 141.29, 150.09, 160.36, 167.69. IR (KBr) 3015 (m), 2990 (m), 1760 (s), 1585–1550 (m), 1205 (m). $[\alpha]_D^{20} = +6.06°$. Elemental analysis for $C_{21}H_{25}N_2O_3Cl$: calc. C 64.86, H 6.44, N 7.21; found C 64.91, H 6.40, N 7.29%.

4. Results and discussion

The chloro and bromo series studied exhibit a simple polymorphism (tables 1 and 2, figure 1). In both series the ferroelectric smectic C* phase is preceded by the paraelectric SmA phase. For short homologues the chiral nematic phase (N*) also appears. Above the chiral nematic phases, relatively broad temperature ranges of blue phases (BP) were detected in microscopic observations, but the phase transitions between the different blue phases were

Table 1. Phase transition temperatures (in °C) and, in parentheses, the enthalpies (J g^{-1}) for the homologous series of chloro compounds.

n	m.p.	SmC*		SmA		N* (BP)		I
3	50.3 (62.8)					•	52.7 (0.7)	•
6	53.2 (65.4)	•	50.7 (0.07)[a]	•	56.0 (0.8)	•	73.6 (1.9)	•
8	57.3 (79.5)			•	60.6 (0.7)	•	70.5 (2.2)	•
9	60.5 (77.0)	•	59.6 (0.3)[a]	•	67.3 (0.5)	•	73.1 (2.6)	•
10	65.6 (87.8)	•	62.2 (0.3)[a]	•	70.4 (0.3)	•	74.3 (5.7)	•
11	46.5 (69.5)	•	68.9 (0.6)	•	76.0 (0.3)	•	77.56 (6.6)	•
12	52.9 (3.8)	•	66.1 (0.3)	•	76.4 (7.2)			•
14	55.0 (77.5)	•	66.0 (0.2)	•	75.4 (7.7)			•
16	62.8 (56.8)	•	72.8 (0.2)	•	78.1 (8.1)			•
18	61.6 (62.9)	•	66.5[b]	•	75.5 (8.5)			•

[a] Monotropic transition.
[b] From microscopic observations.

Table 2. Phase transition temperatures (in °C) and, in parentheses, the enthalpies (J g^{-1}) for the homologous series of bromo compounds.

n	m.p.	SmC*		SmA		N* (BP)		I
10	71.3 (86.0)	•	56.5 (0.2)[a]			•	67.0 (2.4)[a]	•
11	53.6 (67.0)	•	64.1 (0.3)			•	74.3 (4.0)	•
12	56.8 (79.6)	•	65.6 (0.3)			•	74.2 (4.0)	•
14	60.3 (77.8)	•	65.9 (0.3)	•	73.3 (6.79)			•
16	59.4 (60.7)	•	69.4	•	72.5 (6.9)[b]			•

[a] Monotropic transition.
[b] Total enthalpy for SmC*–SmA–I phase transitions.

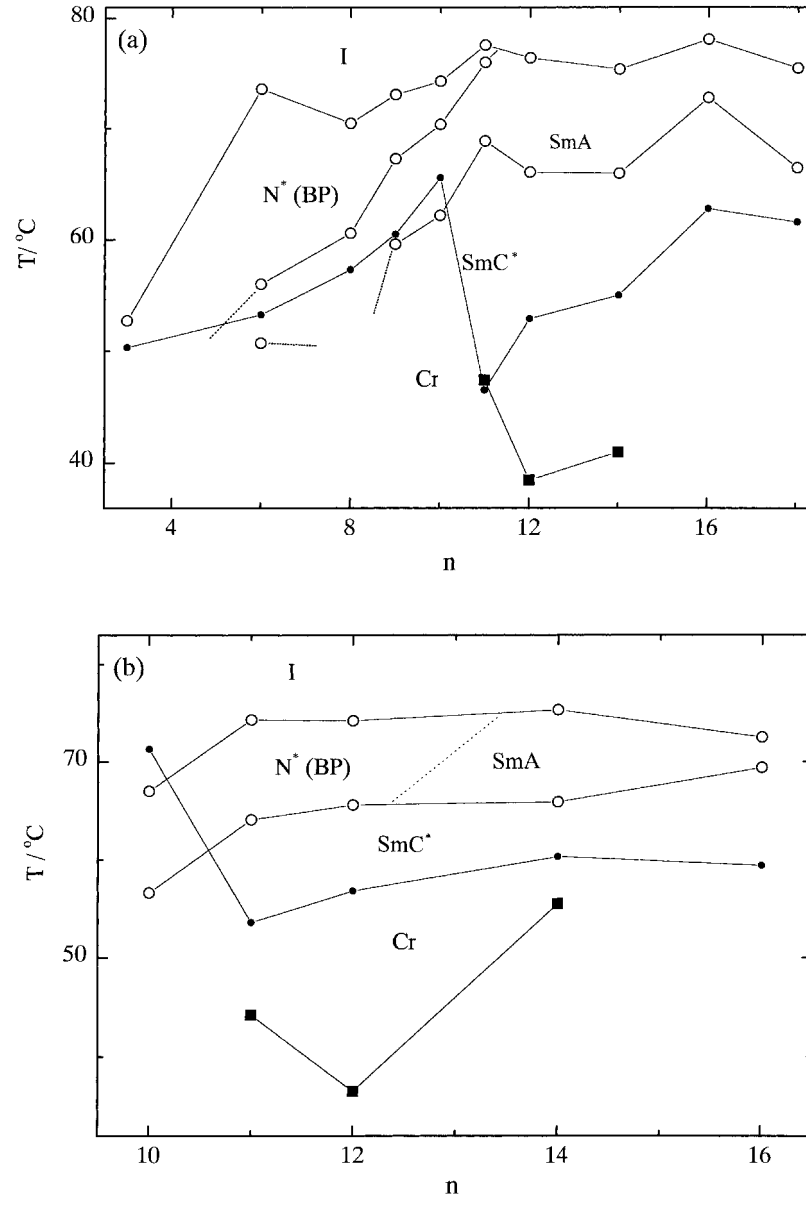

Figure 1. Phase diagram for the series of (*a*) chloro-, (*b*) bromo-derivatives: solid circles are melting points, solids squares are twist inversion points.

not resolved in the calorimetric measurements. For the narrow range nematic phases, the heat capacity anomaly at the nematic–isotropic phase transition influences the heat effects at the subsequent N*–SmA phase transition. The SmA–SmC* phase transition is accompanied by a heat capacity jump or a small transition enthalpy.

The optical tilt angle and the spontaneous polarization measured for the compounds of the chloro series with $n = 6$ and 11 in the SmC* phase do not exhibit any temperature anomaly (figure 2). They continuously increase from zero at the SmA–SmC* phase transition point following the power law. For the tilt angle, the estimated critical exponents are close to the value predicted by the mean field theory with the sixth order term included [9]. The tilt angle amplitude for both compounds approaches about 35° which is rather high for a smectic C* phase preceded by a SmA phase [10]. The critical exponents found for the spontaneous polarization are about 0.45, which might suggest the importance of the non-linear tilt–spontaneous polarization coupling in the mean field free energy expansion [11]. A pronounced electroclinic effect was observed in the SmA phase.

For the *S*,*S*-enantiomers investigated, the sign of the measured spontaneous polarization was negative. This sign of $\mathbf{P}_s(-)$ is in agreement with that predicted on the assumption that, in the mesophase, the molecules are in an all-*trans*-conformation and the molecular core tilt is greater than the tilt of the terminal chains. Transverse dipole moments coming from the electron-accepting halogen and the electron-donati ng methyl group reinforce,

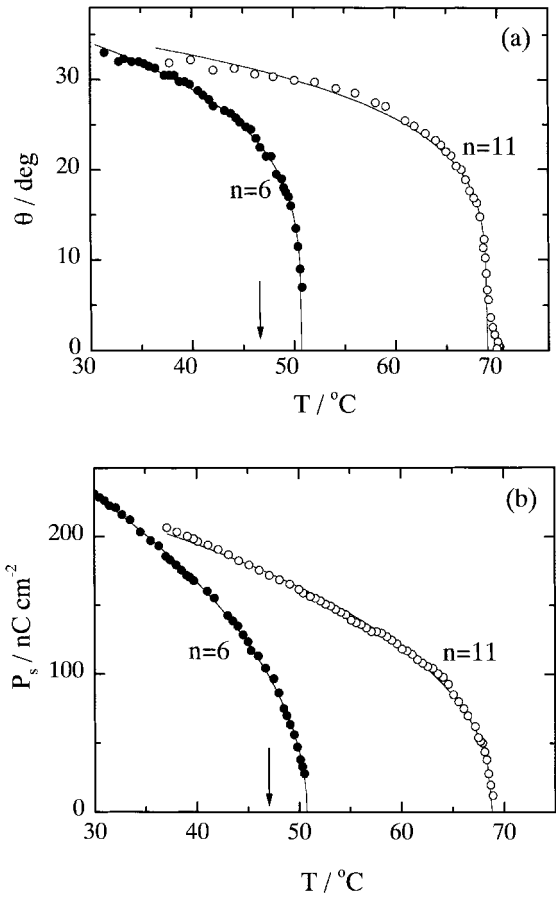

Figure 2. Temperature dependence of (*a*) optical tilt angle, (*b*) spontaneous polarization for the chloro homologues with $n = 6$ and $n = 11$. Measured points for $n = 6$ and 11, are fitted to the power low with the β exponents: for tilt angle $\beta_\theta = 0.20$ and $0.26 + 0.02$, for spontaneous polarization $\beta_p = 0.49$ and 0.41. Arrows indicate the inversion point of the $n = 11$ mesogen.

but the dipole moment of the halogen, which is ten times greater than that of the methyl group, has more influence on the $\mathbf{P}_s$ value. The observed high $\mathbf{P}_s$ value (more than 200 nC cm^{-2} and 150 nC cm^{-2} for the chloro and bromo derivatives, respectively) is also probably caused by steric interactions between the bulky groups at the two chiral centres. They restrict rotational motion of the halogen centre around the molecular axis. Some contribution of the carbonyl dipole to the measured spontaneous polarization should also be considered [8].

For some homologues of the chloro and bromo series, in the chiral SmC* phase, there is observed with changing temperature an unwinding and subsequent rewinding of the helix. The sense of the helix twist is different above and below the temperature of the helix unwinding. The twist inversion points are shown in figure 1. For all compounds that exhibit the helix inversion, the left-handed helix was detected above the inversion temperatures. This handedness of the helical superstructure is in agreement with the modified Gray and McDonnell rules [12, 10] that take into account, besides the spatial configuration and parity of a chiral centre, also the inductive effect of lateral substituents. In our case, the substituents at the two neighbouring chiral centres act in the same way for helix formation, since their induced polarization is opposite: +I for the $-CH_3$ group and − I for Cl or Br substituents.

Below the inversion temperature, the twist sense is reversed and so it seems that in this case the Gray and McDonnell rules are not fulfilled. The lack of visible changes of either the tilt or the spontaneous polarization direction around the helix inversion temperature could suggest that the steric configuration of the halogen remains unchanged over the whole SmC* temperature range. Thus, it might be that there is a variation in conformation of the groups at the second chiral carbon atom $\underline{C}^*H(CH_3)C_2H_5$, which only weakly influences the P_s values. Molecular calculations show that the activation energy necessary fully to rotate a chain fragment around the $-HClC-C(CH_3)H-$ bond is 5–10 kcal mol^{-1}, which is in the range of kinetic thermal energy at relevant temperatures. Probably therefore at temperatures above the helical twist inversion, the conformation of the ethyl chain at the second chiral atom does not remain *trans*, and instead there is free rotation around the $-HClC-C(CH_3)H-$ bond. Below the twist inversion point, where rotation is plausibly restricted, the ethyl chain conformation is not *trans* either, as it has been shown in [8] that the ethyl group has its lowest energy in a *gauche*-conformation. The methyl group then lengthens the terminal chain and the ethyl moiety becomes a quite large lateral substituent. In this low energy position, the ethyl group with its positive inductive effect (+I) can induce the helical structure in the opposite way to the halogen substituent. The competition between the steric interaction of the two lateral substituents (halogen and ethyl) then results in the left- or right-handed helix formation. At lower temperatures, the larger ethyl group seems to be more influential and the right twisted helical superstructure appears. It may be supposed that for compounds with a longer terminal chain, the inversion of the helical twist will not be observed. In this case a stable arrangement of the alkyl chain in the *gauche*-conformation would be less probable.

A few compounds of the chloro series (with $n = 6$, 9, 10 and 16) do not exhibit the helix inversion phenomenon; the left-handed helix is detected over the whole SmC* temperature range. For these homologues, the twist inversion points are probably below the recrystallization points. For short terminal chain compounds ($n = 6$–11), just below the phase transition SmA–SmC*, the helical

pitch is very short (below 1 μm) and for samples as homeotropic freely suspended films, a small optical rotation is observed [1, 3]. For long chain homologues the helix pitch is found to be longer (above a few μm). Moreover, the compound with $n = 14$, which exhibits inversion, scarcely reforms the helix below the unwinding point; the compound with $n = 16$ does not form a helix in a glass plate cell; and the longest homologue with $n = 18$ reveals a non-twisted smectic C phase. Similar effects are present in the bromo series. For both series, the ability to create helical superstructure in the SmC* phase decreases upon elongation of the terminal alkyl chain.

In the compounds studied, the dielectric permittivity measurements showed a strong soft mode in the SmA phase. In the SmC* phase only the Goldstone mode was detected with a relaxation frequency f_r around 500 Hz. For the chloro compound ($n = 6$) without helix inversion, the Goldstone mode strength $\Delta\varepsilon$ and relaxation frequency f_r measured in a planar sample are, as usual, only weakly temperature-dependent (figure 3).

In the homologues that give the helix unwinding, both the relaxation frequency and the dielectric strength of the Goldstone mode exhibit a strong anomaly in the vicinity of the twist inversion temperature (figure 4). For the chloro mesogen with $n = 11$ as a freely suspended film, the measurements show a very low relaxation frequency at the unwinding point. Around this temperature, the relaxation frequency goes below 20 Hz, the experimental limit of our apparatus. At such a low value, the parameters f_r and $\Delta\varepsilon$ were determined in the fitting procedure based on data which covered only a part of the Cole–Cole dispersion curve. The results display a gradual decrease of the relaxation frequency upon approaching the unwinding temperature. This is accompanied by a very strong increase in the mode strength $\Delta\varepsilon$ (figure 5). Although the accuracy of determination of the curve parameter around the inversion is rather poor, it seems that in the film sample, the helix unwinding temperature corresponds to the maximum Goldstone mode strength and to the minimum relaxation frequency.

The data obtained for a planar sample give a more complicated temperature dependence of the dielectric mode parameters (figure 5). On cooling, the Goldstone mode relaxation frequency decreases by a factor of two around the unwinding temperature, while in the homeotropic geometry it drops more than ten times [14]. Below this point the f_r value remains at a constant low level. The maximum of the relaxation mode strength $\Delta\varepsilon$ is smaller and appears above the inversion temperature. In consecutive heating runs, a strong hysteresis of the dielectric properties was observed; both the f_r and $\Delta\varepsilon$ values do not recover and remain at low values up to the SmA phase. This points to some difficulties in

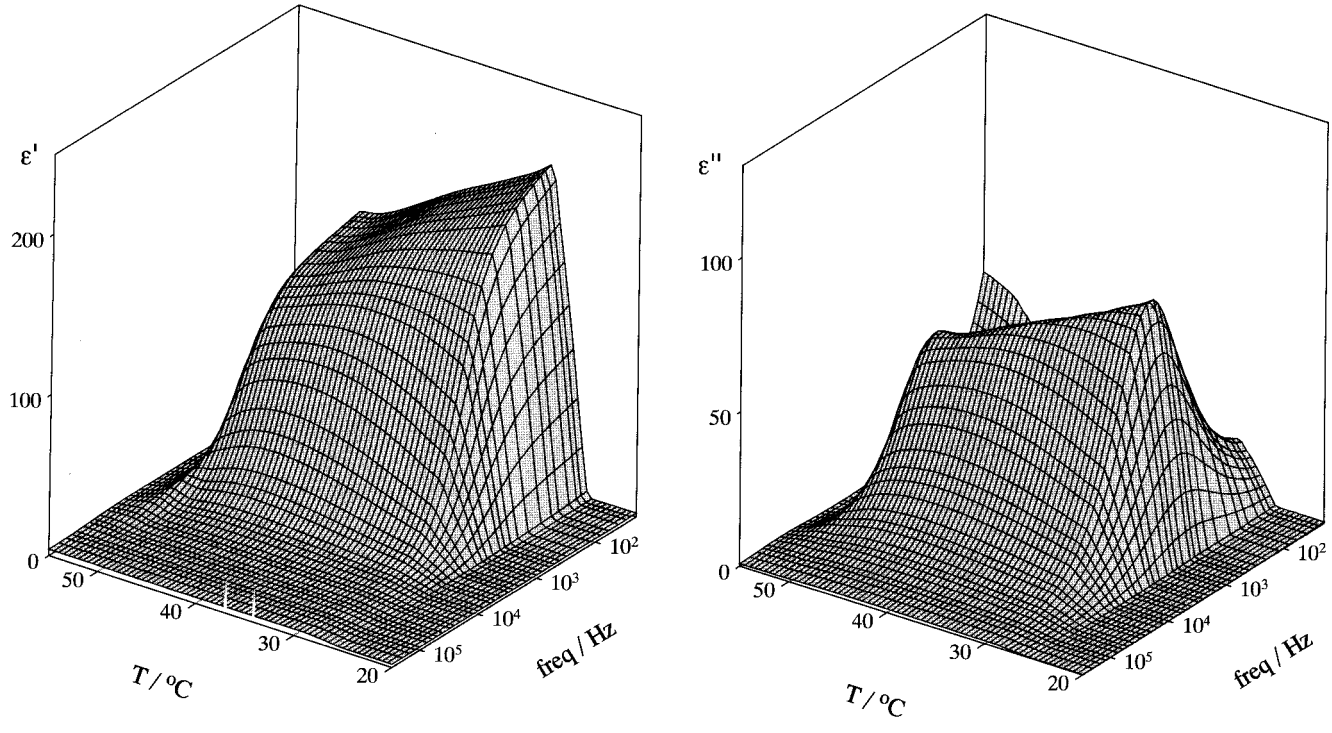

Figure 3. Surface temperature–frequency plots of the real and imaginary dielectric permittivity measured on cooling in planar aligned glass cells for the chloro homologue with $n = 6$.

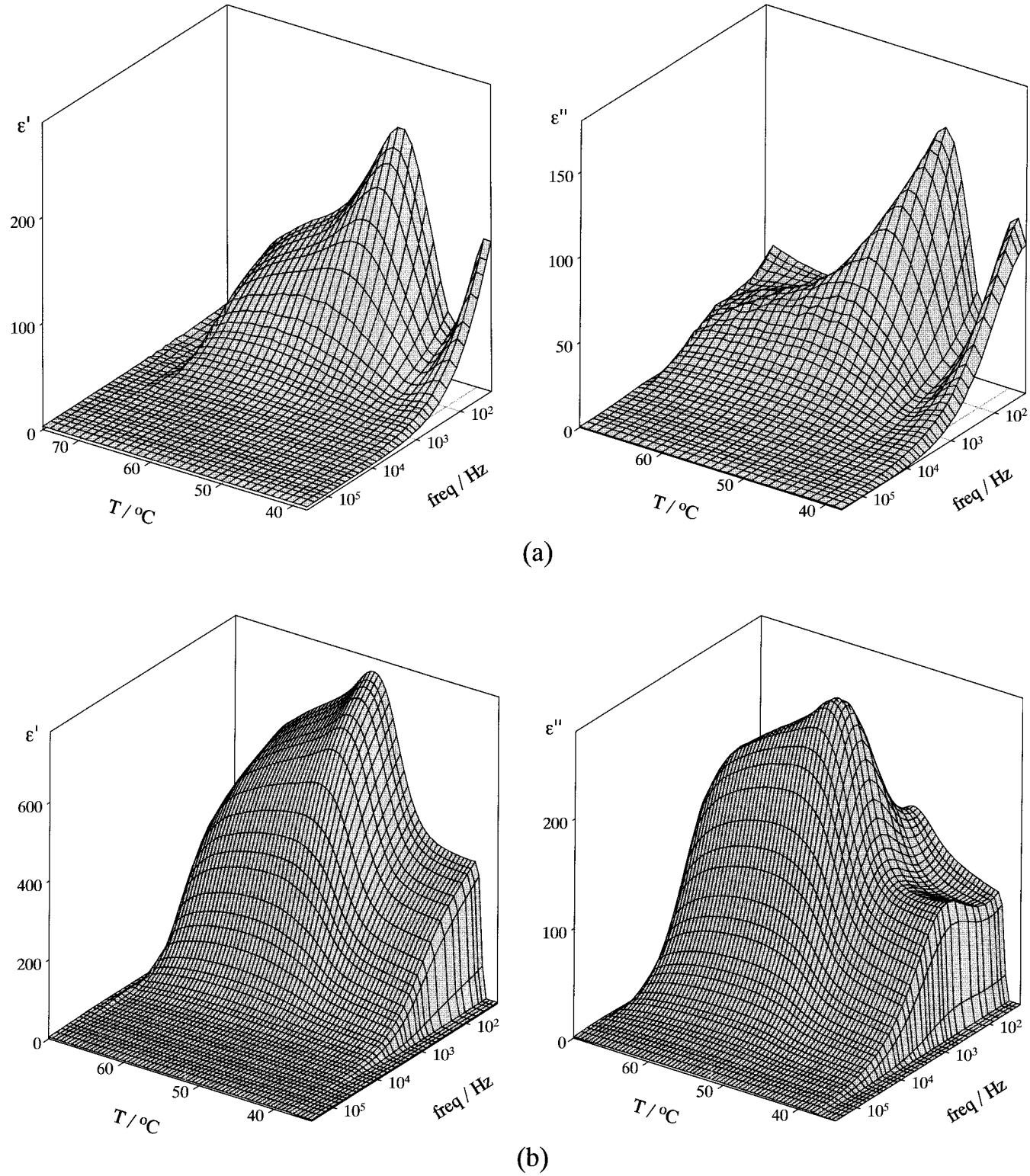

Figure 4. Surface temperature–frequency plots of the real and imaginary dielectric constant measured on cooling for the chloro homologue with $n = 11$ as (*a*) a freely suspended film, (*b*) a planar sample.

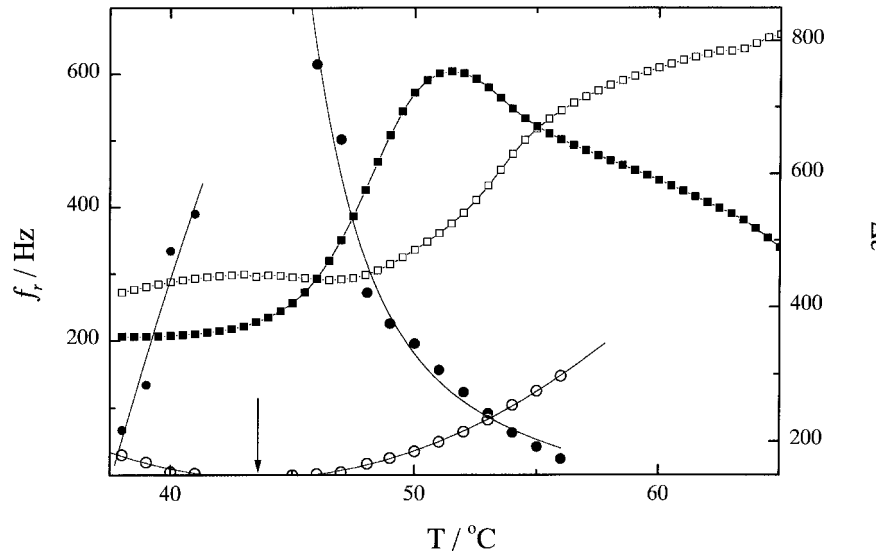

Figure 5. Temperature dependence of the relaxation frequency (open symbols) and strength (solid symbols) of the Goldstone mode for the chloro homologue with $n = 11$ examined as freely suspended film samples (circles) and planar samples (squares). The arrow indicates the helix inversion temperature. Lines are only guides for the eye.

restoring the helix for the planar sample, a fact confirmed by texture observations. On cooling, the dechiralization lines gradually disappear and they do not reform either after passing the unwinding temperature or on consecutive heating. The observed differences in behaviour of the Goldstone mode in homeotropic and homogeneous samples come from the different anchoring energy of molecules on the surface of the freely suspended film and the planar surfactant coated glass plates [15, 14]. For the planar sample, the strong molecular anchoring gives a twisted structure along a normal to the sample plane [16]. As a result, in the dielectric measurements a thickness mode appears, which interferes with the Goldstone mode. Thus both the Goldstone and thickness modes influence the measured dielectric permittivity. For the samples, where the dechiralization lines disappear, the twisted structure induced by the surface anchoring is present and only the pure twisted mode is probably observed.

5. Conclusions

Both series of chloro and bromo homologues form the chiral smectic C* phase and the helix inversion phenomenon was found for compounds of intermediate molecular length. For short and long homologues, the twist inversion points seem to be below the freezing temperatures. At higher temperatures, the helix sense is identical for all compounds. The long pitch helix created by the long chain homologues is easily destroyed even by anchoring to the glass surface.

The helix inversion interferes with neither the molecular tilt value nor the sign of the spontaneous polarization; both parameters smoothly follow the temperature changes. The structure of the helix can be described by the Gray and McDonnell rules for the upper SmC* temperature range exclusively. Below the twist inversion point, the sign of the spontaneous polarization, the direction of the transverse molecular dipole moment and the sense of the helical twist contradict each other. It seems that molecular rather than thermodynamic factors should be considered as responsible for the appearance of the helix twist inversion phenomenon [5]. The changes of conformation at the second chiral centre, substituted by the methyl group, are crucial for the twist sense inversion.

The helix unwinding was found to play a significant role in the collective fluctuations of the tilt angle—the Goldstone mode. When measured for a freely suspended film, the relaxation frequency f_r has a deep minimum and the dielectric strength $\Delta\varepsilon$ exhibits a large maximum at the helix unwinding point. The similar dependence of the relaxation frequency and dielectric strength on helical pitch has already been theoretically predicted [4]. The measurements also show a significant influence of surface interactions on the appearance of the helix and thereby on the measured dielectric permittivity. On the planar geometry, a temperature hysteresis of the dielectric parameters was observed.

The synthetic work was supported by UW grant BW-1383/21/97 and the physical studies by KBN grant 3 T09A 046 15. D.P. wishes to acknowledge a Scholarship from the Foundation for Polish Sciences.

References

[1] Kaspar, M., Gorecka, E., Sverenyak, H., Hamplova, V., Glogarova, M., and Pakhomov, S. A., 1995, *Liq. Cryst.*, **19,** 589.

[2] Styring, P., Vuijk, J. D., Wright, S. A., Takatoh, K., and Dong, Ch., 1994, *J. mater. Chem.*, **4,** 1365.

[3] MARTINOT-LAGARDE, PH., DUKE, R., and DURAND, G., 1981, *Mol. Cryst. liq. Cryst.*, **75,** 249.
[4] ZEKS, B., and BLINC, R., 1991, in *Ferroelectric Liquid Crystals*, edited by J. W. Goodby *et al.* (Philadelphia: Gordon and Breach Science publications).
[5] GORECKA, E., GLOGAROVA, M., SWERENYAK, H., KASPAR, M., HAMPLOVA, V., and PAKHOMOV, S. A., 1996, *Ferroelectrics*, **179,** 81.
[6] GOODBY, J. W., STYRING, P., SLANEY, A. J., VUIJK, J. D., PATEL, J. S., LOUBSER, C., and WESSEL, P. L., 1993, *Ferroelectrics*, **147,** 291.
[7] GLOGAROVA, M., LEICEK, M., PAVEL, L., JANOVEC, J., and FOUSEK, J., 1983, *Mol. Cryst. liq. Cryst.*, **91,** 309.
[8] SIERRA, T., SERRANO, J. L., ROS, M. B., EZCURRA, A., and ZUBIA, J., 1992, *J. Am. chem. Soc.*, **114,** 7645.
[9] HUANG, C. C., and VINER, J. M., 1982, *Phys. Rev. A*, **25,** 3385.
[10] GOODBY, J. W., 1991, in *Ferroelectric Liquid Crystals*, edited by J. W. Goodby *et al.* (Philadelphia: Gordon and Breach Science publications).
[11] BLINC, R., 1992, in *Phase Transitions in Liquid Crystals*, edited by S. Martellucci *et al.* (New York: Plenum Press).
[12] GRAY, G. W., and MCDONNELL, D. G., 1977, *Mol. Cryst. liq. Cryst. Lett.*, **34,** 211.
[13] DE VRIES, H., 1951, *Acta Crystallogr.*, **90,** 333; DE GENNES, P. G., and PROSE, J., 1995, *The Physics of Liquid Crystals*, 2nd Edn (Oxford: Clarendon Press).
[14] GLOGAROVA, M., SVERENYAK, H., HOLAKOVSKY, J., NGUYEN, H. T., and DESTRADE, C., 1995, *Mol. Cryst. liq. Cryst.*, **263,** 245.
[15] GLOGAROVA, M., and PAVEL, J., 1984, *Mol. Cryst. liq. Cryst.*, **114,** 249.
[16] GLOGAROVA, M., LEJCEK, L., PAVEL, J., JANOVEC, V., and FONSEK, J., 1983, *Mol. Cryst. liq. Cryst.*, **91,** 309.